EFFECT OF IMMERSION TIME ON THE ELECTROCHEMICAL BEHAVIOUR OF AISI 321 STAINLESS STEEL IN 0.1 M H$_2$SO$_4$ SOLUTION

A. Fattah-alhosseini* and O. Imantalab

* a.fattah@basu.ac.ir

Faculty of Engineering, Bu-Ali Sina University, Hamedan, Iran.

Abstract: *In this study, effect of immersion time on the electrochemical behaviour of AISI 321 stainless steel (AISI 321) in 0.1 M H$_2$SO$_4$ solution under open circuit potential (OCP) conditions was evaluated by potentiodynamic polarization, Mott–Schottky analysis and electrochemical impedance spectroscopy (EIS). Mott–Schottky analysis revealed that the passive films behave as n-type and p-type semiconductors at potentials below and above the flat band potential, respectively. Also, Mott–Schottky analysis indicated that the donor and acceptor densities are in the range 1021 cm-3 and increased with the immersion time. EIS results showed that the best equivalent circuit presents two time constants: The high-medium frequencies time constant can be correlated with the charge transfer process and the low frequencies time constant has been associated with the redox processes taking place in the surface film. According to this equivalent circuit, the polarization resistance (interfacial impedance) initially increases with the immersion time (1 to 12 h), and then it is observed to decreases. This variation is fully accordance with potentiodynamic polarization results.*

Keywords: Stainless steel; immersion time; Mott–Schottky; Equivalent circuit.

1. INTRODUCTION

Austenitic stainless steels (especially AISI 321) are the most common of the multi-component construction materials used by the chemical and petrochemical industries. These steels are selected basically for a good combination of mechanical, fabrication and corrosion resistance properties [1-3]. Generally, the higher corrosion resistance of stainless steel is due to the presence of a very thin passivating and self-renewable protective layer (passive films) formed on the surface [4, 5].

These passive films are mainly made up of metallic oxides or hydroxides which are envisaged as semiconductors. Consequently, semiconducting properties are often observed on the surfaces of the passivity metals. Their electrical properties are expected to be crucially important in understanding the protective characters against corrosion. Mott–Schottky analysis has been widely used to study the semiconducting properties of the passive films, such as the passive films on chromium [6], nickel [7], aluminum [8], titanium [9] and carbon steels [10].

In the last decade, increasing research of the electronic properties of passive films formed on stainless steels has given an important contribution to the understanding of the corrosion behaviour of these alloys [11-13]. Depending on the predominant defects present in the passive oxide layer on stainless steels, either p-type or n-type behaviours are observed. The passive oxide films with a deficiency in metal ions or excess with cation vacancies generally behave as p-type. Similarly, n-type is developed in the passive films either by excess cation in interstitial sites or anion vacancies. Mott–Schottky analysis has been shown to be an important in-situ method for investigation of the semiconductor properties of passive films [14].

The electrochemical behaviour of the passive films on stainless steels is an important factor, which control the passivity and, therefore, the corrosion resistance. This behaviour are dependent on several variables, including the chemical composition of the steel, temperature, immersion time, pH and composition of the electrolyte in which the films are grown [15-17]. There are also several interesting studies focused on the corrosion and passivation behaviour of the

passive film formed in solutions simulating concrete of stainless steel [18, 19].

Although many models and theories have been proposed to explain the passivation of materials, a satisfactory description of the phenomenon is still in lack. The Point defect model (PDM) [20], which was developed by Macdonald et al., described the growth and breakdown of passive film qualitatively from a microscopic perspective. This model is based on the assumption that the passive film contains a high concentration of point defects, such as oxygen vacancies and metal cation vacancies. The growth and breakdown of the passive film involves the migration of these point defects under the influence of the electrostatic field in the film. Thus, the key parameters in determining the transport of point defects and hence the kinetics of film growth is the density of the defects in film.

However, there are limited systematic studies on the effects of the immersion time on the passive behaviour of stainless steel in acidic solutions. The aim of this paper was to investigate the influence of the immersion time in 0.1 M H_2SO_4 solution on the AISI 321 under OCP conditions using the potentiodynamic polarization and EIS. Also, Mott-Schottky analysis of AISI 321 in 0.1 M H_2SO_4 solution was performed and the defects concentrations were calculated as a function of the immersion time. The relationship between the defects concentrations and the immersion time are discussed in order to understand the property of the passivation of AISI 321.

2. EXPERIMENTAL PROCEDURES

Specimens were fabricated from 14 mm diameter rods of AISI 321 with the chemical composition (%, wt.): 19.1 Cr, 9.85 Ni, 1.65 Mn, 0.16 Mo, 0.29 Si, 0.68 Ti, 0.05 S, 0.08 C. The samples were placed in stainless steel sacks and annealed in inert environment (Ar gas) to eliminate the cold work effect due to cutting process. The annealing was performed at 1050 °C for 1 h followed by water quenching [20]. All samples were polished mechanically by abrading with wet emery paper up to 1200 grit size on all

sides and then were embedded in cold curing epoxy resin. After this, the stainless steels were degreased with acetone, rinsed with distilled water and dried with a stream of air just before immersion. The solution (0.1 M H_2SO_4) was prepared from analytical grade 97% H_2SO_4 and distilled water, and the tests were carried out at ambient temperature.

All electrochemical measurements were performed in a conventional three-electrode cell under aerated conditions. The counter electrode was a Pt plate, and all potentials were measured against Ag/AgCl in saturated KCl. All electrochemical measurements were obtained using μautolab potentiostat/galvanostat controlled by a personal computer.
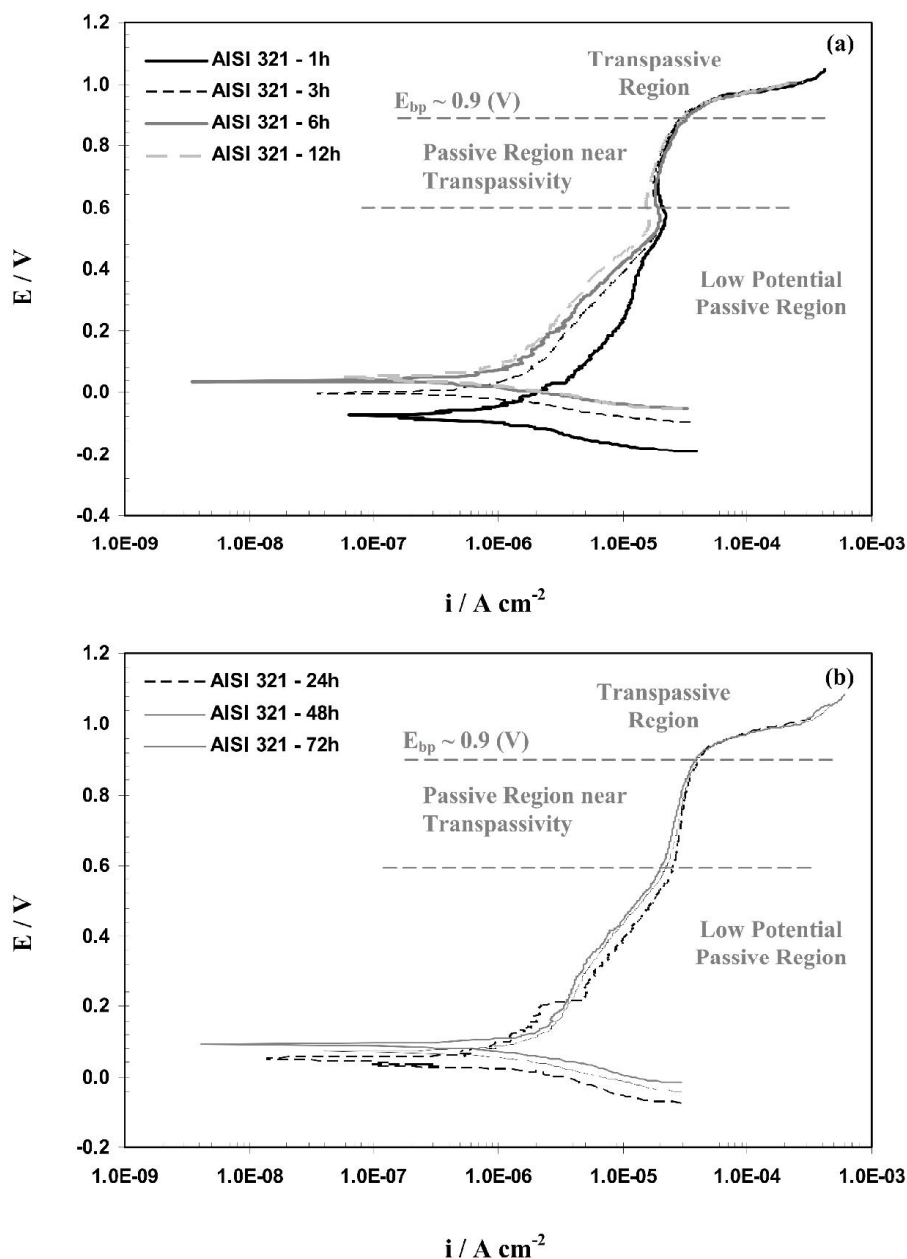
Potentiodynamic polarization curves were measured potentiodynamically at a scan rate of 1 mV/s. The impedance spectra were measured in a frequency range of 10 mHz −100 KHz at an AC amplitude of 10 mV (rms). The validation of the impedance spectra was performed by checking the linearity condition, i.e. measuring spectra at AC signal amplitudes between 5 and 15 mV (rms) [20]. Each electrochemical measurement was repeated at least three times. For EIS data modeling and curve-fitting method, NOVA impedance software was used.

Capacitance measurements were carried out on the passive films formed by immersion in the acidic solution for different immersion times from 1 to 72 h. The capacitance tests were performed at a frequency of 1 kHz using a 10 mV ac signal and a step rate of 25 mV, in the cathodic direction [20].

3. RESULTS AND DISCUSSION

3. 1. Potentiodynamic Polarization

Fig. 1(a) and (b) shows the potentiodynamic polarization curves of AISI 321 immersed in 0.1 M H_2SO_4 solution from 1 to 72 h. According to Fig. 1(a) and (b), two stages of the passive process can be distinguished for all potentiodynamic polarization curves. The low potential passive region ranges from about corrosion potential to 0.6V. In passive region near transpassivity, the comparatively slow increase of

Fig. 1. Potentiodynamic polarization curves at 1 mV/s for AISI 321 in 0.1 M H2SO4 solution after different immersion times: (a) 1 to 12 h and (b) 24 to 72 h.

the current in the potential range 0.6–0.9V could be connected to the formation of high valency Cr in the film prior to transpassive dissolution [21]. The steeper increase in transpassive region is most probably related to the onset of the transpassive dissolution.

According to Fig. 1(a) and (b), by comparing the polarization curves, the corrosion potentials were found to shift slightly towards positive direction with an increase in the immersion time. For all curves, the current decreased with potential during the early stage of passivation and no obvious current peak was observed. It can be found that the passive currents decreased with the immersion time. Also, all curves exhibit similar features, with a passive potential range extending from the corrosion potential to the onset of transpassivity. Table 1 summarizes the corrosion

Table 1. Passivation values of AISI 321 immersed in 0.1 M H$_2$SO$_4$ solution at different immersion times.

Time (h)	E_{corr} (V)	i_{corr} ($\mu A\ cm^{-2}$)
1	-0.074	2.1
3	-0.002	1.7
6	0.034	1.3
12	0.048	0.7
24	0.053	1.0
48	0.071	1.2
72	0.093	1.6

potential and corrosion current density of AISI 321 immersed in 0.1 M H$_2$SO$_4$ solution from 1 to 72 h. As shown in this table, corrosion current density initially decreased with the immersion time, 1 to 12 h, due to the establishment of the passive film layer. At the sufficiently immersion time (t >12 h), the corrosion current density is observed to increase with increasing time.

3. 2. Mott-Schottky Analysis

The previous study has proved that the outer layer of passive films contains the space charge layer and sustains a potential drop across the film. The charge distribution at the semiconductor /solution is usually determined based on Mott-Schottky relationship by measuring electrode capacitance C, as a function of electrode potential E [22, 23]:

$$\frac{1}{C^2} = \frac{2}{\varepsilon \varepsilon_0 e N_D}\left(E - E_{FB} - \frac{kT}{e}\right) \quad \text{for n-type semiconductor}$$
(1)

$$\frac{1}{C^2} = -\frac{2}{\varepsilon \varepsilon_0 e N_A}\left(E - E_{FB} - \frac{kT}{e}\right) \quad \text{for p-type semiconductor}$$
(2)

where e is the electron charge (-1.602×10^{-19} C),), N$_D$ is the donor density for n–type semiconductor (cm^{-3}), N$_A$ is the accept density for p–type semiconductor (cm^{-3}), ε is the dielectric constant of the passive film, usually taken as 15.6 [20, 24]), ε$_0$ is the vacuum permittivity (8.854×10^{-14} F cm^{-1}), k is the Boltzmann constant (1.38×10^{-23} J K^{-1}), T is the absolute temperature and E_{FB} is the flat band potential. From Eq. (1) N_D can be determined from the slope of the experimental C^{-2} versus E plots, and E_{FB} from the extrapolation of the linear portion to C^{-2} = 0. The validity of Mott-Schottky analysis is based on the assumption that the capacitance of the space charge layer is much smaller than the double layer capacitance. Hence, the capacitance determined is mainly from the contribution of the space charge layer. This assumption is reasonable provided that the frequency is high enough [20].

Fig. 2(a) and (b) shows the Mott-Schottky plots of AISI 321 immersed in 0.1 M H$_2$SO$_4$ solution from 1 to 72 h. Firstly, it should be noted that for all immersion times, capacitances clearly decrease with time. This trend is consistent with the results of the polarization curves. Secondly, all plots show three regions in which a linear relationship between C^{-2} and E can be observed. The negative slopes in region I are attributed to a p-type behaviour, probably due to the presence of Cr$_2$O$_3$, FeO and NiO on the passive films [25]. Region II presents positive slopes, which depicts an n-type semiconducting behaviour. Finally, the negative slopes in region III are attributed to p-type behaviour, with a peak at around 0.6 V. This feature is usually explained in terms of a strong dependence of the Faradaic current on potential in the transpassive region [25]. In this sense, the behaviour of capacitance at high potentials near the transpassive region is attributed to the development of an inversion layer as a result of an increasing concentration in the valence band (high valency Cr in the film prior to transpassive dissolution). This is consistent with the results obtained from the polarization curve, in which the passive region near transpassivity for all

immersion times was found to be close in the potential range 0.6–0.9V [21].

In all plots, straight lines with a negative and positive slope separated by a narrow potential plateau region (−0.1 to 0.1 V), where the flat band potential (Efb) is observed. In the potential more than −0.1 V, the positive slope indicates n-

type behavior and in the potential less than −0.1 V, the negative slope is representative of the behavior of a p-type behavior. Thus, Mott-Schottky analysis show that the passive films formed on this stainless steel behave as n-type and p-type semiconductors above and below the flat band potential, respectively. This behavior
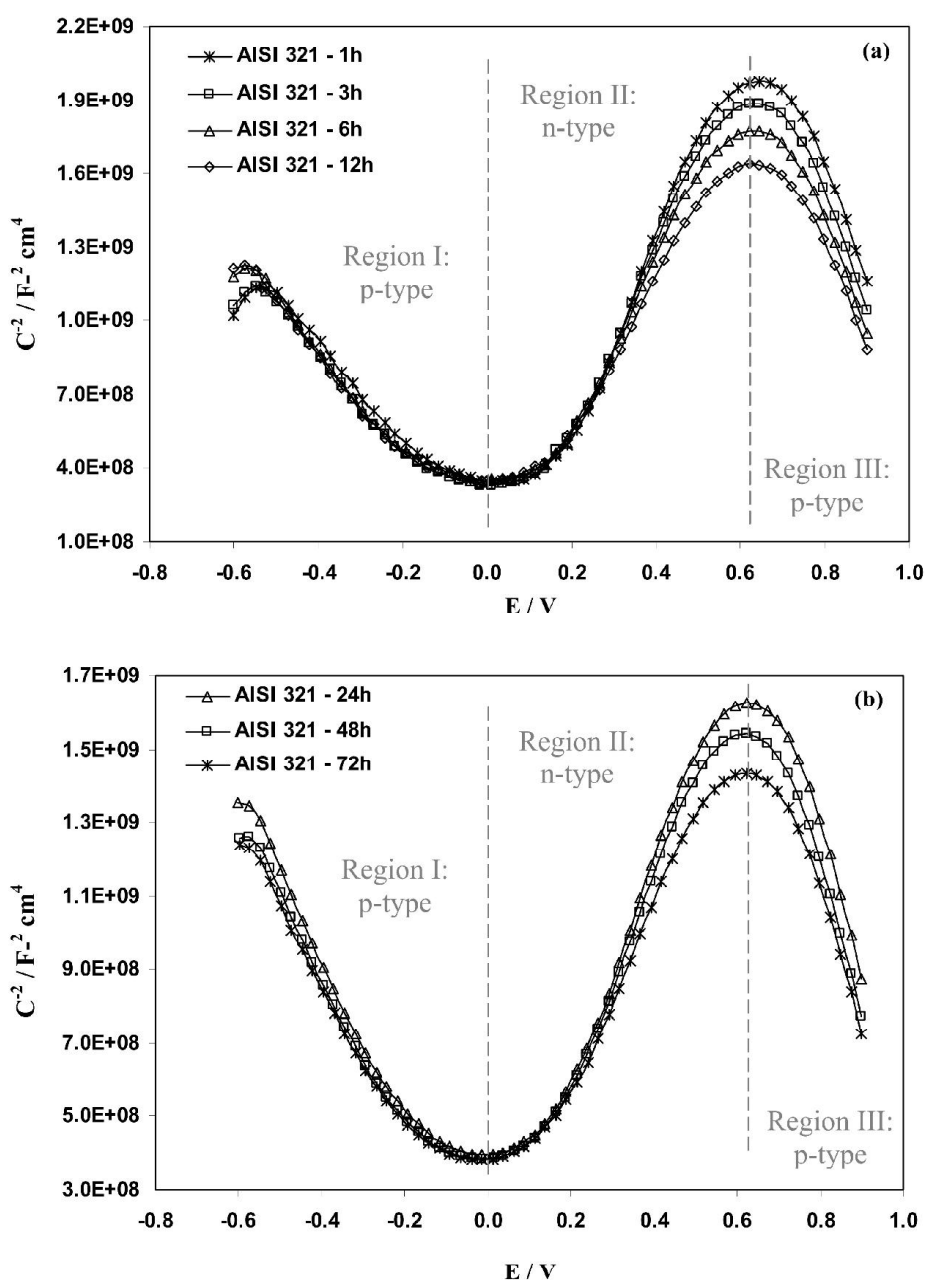

Fig. 2. Mott-Schottky plots of AISI 321 in 0.1 M H2SO4 solution after different immersion times: (a) 1 to 12 h and (b) 24 to 72 h.

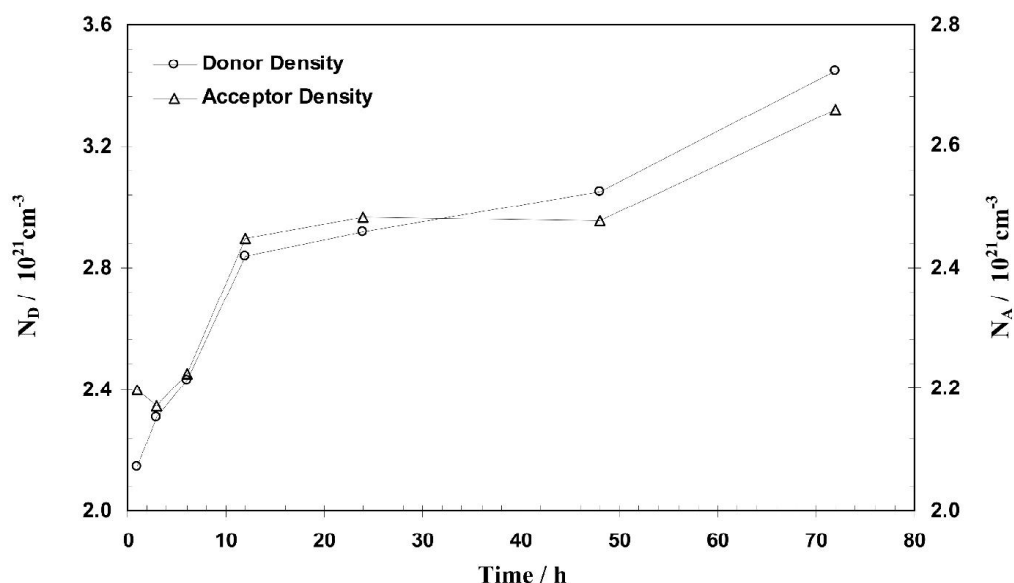**Fig. 3.** Donor and acceptor densities of the passive films formed on AISI 321 in 0.1 M H_2SO_4 solution after different immersion times.
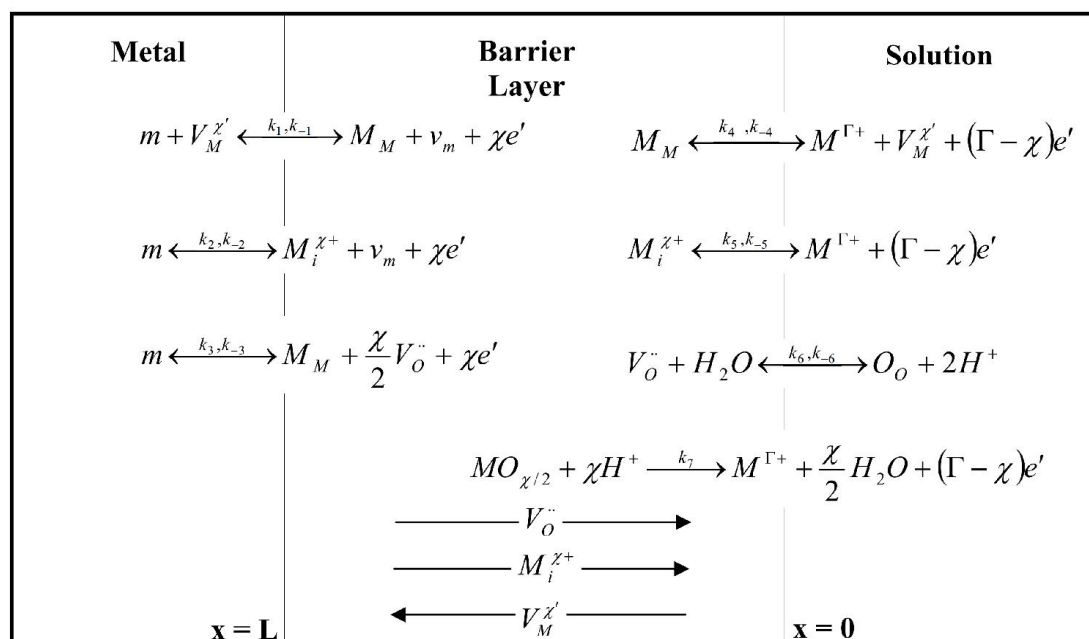
implies that the passive films have a duplex structure, which would not have been realized if the measurements were restricted to only the more anodic potentials. Early studies of the bipolar duplex structures of passive films on stainless steels are attributed to Sato [26], and since then, other investigations have given credence to this observation [27, 28]. It is widely accepted that the inner part of the passive film, which has a p-type behavior, consists mainly of Cr oxides, whereas the outer region, with the features of an n-type behavior, is predominantly Fe oxides. Contributions to the p-type behavior at E < Efb are restricted to the inner Cr oxide layer, with negligible contributions from the Fe oxides in the outer part of the film, whereas the n-type behavior at E > Efb depends exclusively on the outer Fe oxide region with no contribution from the Cr oxide region [28].

According to Eq. (1), donor density has been determined from the positive slopes in region II of Fig. 2(a) and (b). Also, acceptor density has been calculated from the negative slopes in region III of Fig. 2(a) and (b), according to Eq. (2). Fig. 3 shows the calculated donor and acceptor densities for the films formed on AISI 321 immersed in 0.1 M H_2SO_4 solution from 1 to

72 h. The orders of magnitude are around 1021 cm^{-3} and are comparable to those reported in other studies [20, 28]. According to Fig. 3, the donor and acceptor densities increase with the immersion time. Changes in donor and acceptor densities correspond to the non-stoichiometry defects in the passive film. Therefore, it can be concluded that the passive film on AISI 321 is disordered and becomes more visible at higher immersion time. Based on PDM the donors or acceptors in semiconducting passive layers are point defects, as explained briefly in the part 3. 3.

3. 3. Point Defect Model

The PDM [29] postulates that passive films are bilayer structures comprising a highly defective barrier layer that grows into the metal and an outer layer that forms via the hydrolysis of cations transmitted through the barrier layer and the subsequent precipitation of a hydroxide, oxyhydroxide, or oxide, depending upon the formation conditions. The outer layer may also form by transformation of the outer surface of the barrier layer itself, provided that the outer layer is thermodynamically more stable than the barrier layer.

62

Metal	Barrier Layer	Solution
$m + V_M^{\chi'} \xleftrightarrow{k_1,k_{-1}} M_M + v_m + \chi e'$		$M_M \xleftrightarrow{k_4,k_{-4}} M^{\Gamma+} + V_M^{\chi'} + (\Gamma - \chi)e'$
$m \xrightarrow{k_2,k_{-2}} M_i^{\chi+} + v_m + \chi e'$		$M_i^{\chi+} \xleftrightarrow{k_5,k_{-5}} M^{\Gamma+} + (\Gamma - \chi)e'$
$m \xrightarrow{k_3,k_{-3}} M_M + \dfrac{\chi}{2} V_O^{\cdot\cdot} + \chi e'$		$V_O^{\cdot\cdot} + H_2O \xleftrightarrow{k_6,k_{-6}} O_O + 2H^+$

$$MO_{\chi/2} + \chi H^+ \xrightarrow{k_7} M^{\Gamma+} + \frac{\chi}{2} H_2O + (\Gamma - \chi)e'$$

$$\xrightarrow{\quad\quad V_O^{\cdot\cdot} \quad\quad}$$
$$\xrightarrow{\quad\quad M_i^{\chi+} \quad\quad}$$
$$\xleftarrow{\quad\quad V_M^{\chi'} \quad\quad}$$

x = L   x = 0

Fig. 4. Interfacial defect generation-annihilation reactions that are postulated to occur in the growth of passive films according to the PDM. m = metal atom, = metal cation on the metal sublattice, = oxygen anion on the oxygen sublattice, = metal cation in solution [29].

The PDM further postulates that the point defects present in a barrier layer are, in general, cation vacancies (V_M^{χ}), oxygen vacancies ($V_O^{\cdot\cdot}$), and cation interstitials ($M_i^{\chi+}$), as designated by the Kroger-Vink notation. The defect structure of the barrier layer can be understood in terms of the set of defect generation and annihilation reactions occurring at the metal/barrier layer interface and at the barrier layer- solution interface, as depicted in Fig. 4 [29].

Cation vacancies are electron acceptors, thereby doping the barrier layer p-type, whereas oxygen vacancies and metal interstitials are electron donors, resulting in n-type doping. Thus, on pure metals, the barrier layer is essentially a highly doped, defect semiconductor, as demonstrated by Mott-Schottky analysis, for example. Not unexpectedly, the situation with regard to alloys is somewhat more complicated than that for the pure metals, because substitution of other metal cations, having oxidation states different from the host, on the cation sublattice may also impact the electronic defect structure of the film. Thus, while the barrier layers on pure chromium and on Fe-Cr-Ni alloys are commonly described as being "defective Cr_2O_3," that on pure chromium is normally p-type in electronic character, while those on the stainless steels are n-type. It is not known whether this difference is due to doping of the barrier layer by other alloying elements (Ni, Fe), as indicated above, or is due to the inhibition of cation vacancy generation relative to the generation of oxygen vacancies and metal interstitials, in the barrier layer on the alloys compared with that on pure chromium [29].

According to the PDM, the flux of oxygen vacancy and/or cation interstitials (Cr^{2+}, Cr^{3+}, Fe^{2+}, and Ni^{2+}) through the passive film is essential to the film growth process [20]. In this concept, the dominant point defects in the passive film at low potential passive region are considered to be oxygen vacancies and/or cation interstitials acting as electron donors.

3. 4. EIS Measurements

Fig. 5(a) and (b) presents the EIS spectra of AISI 321 immersed in 0.1 M H_2SO_4 solution at OCP conditions from 1 to 72 h. All Nyquist plots
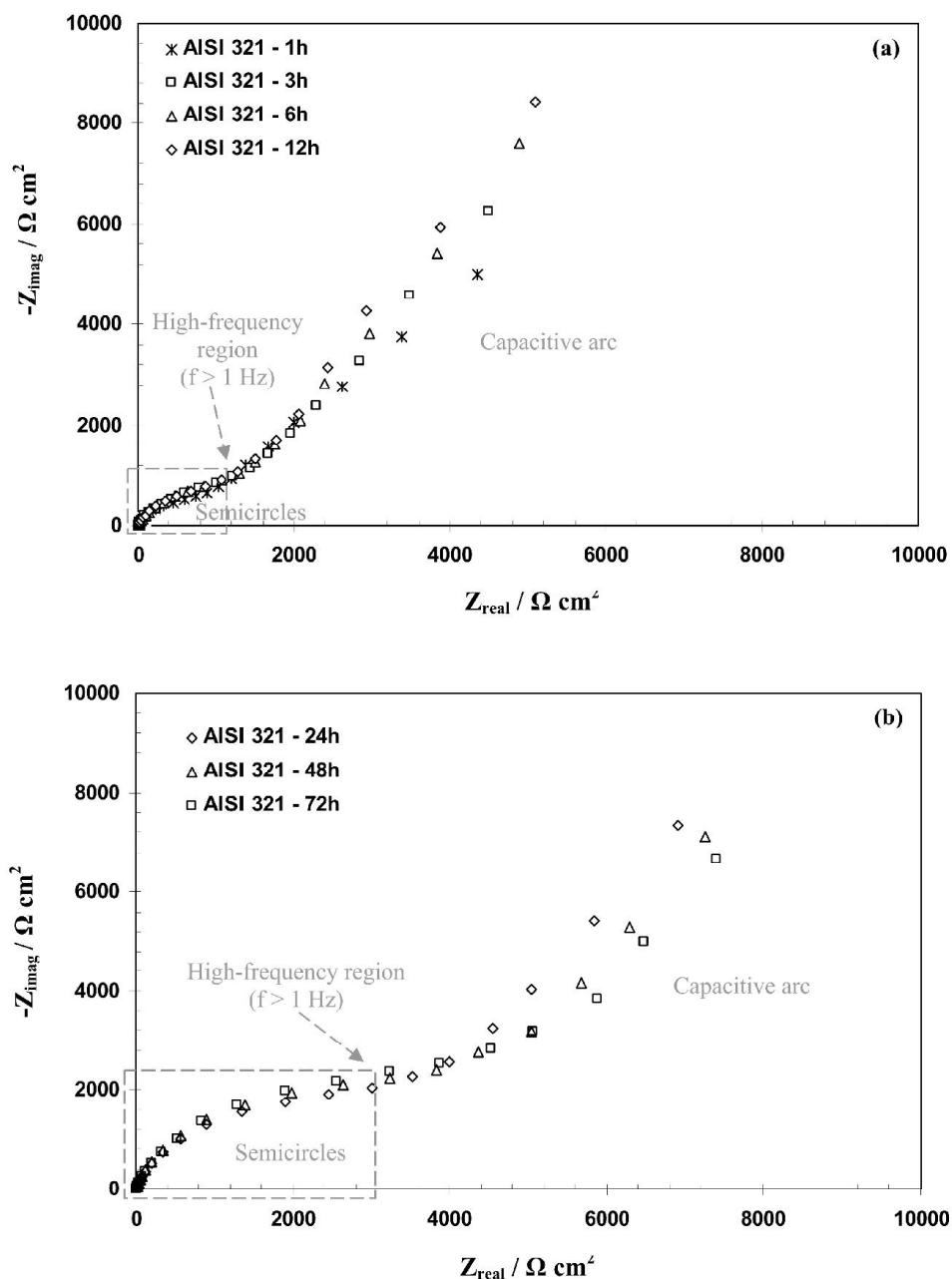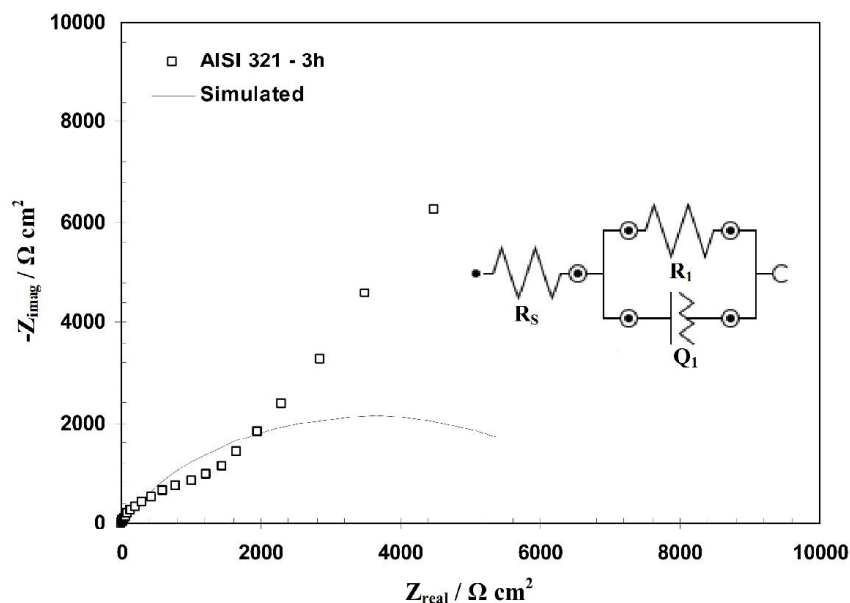
Fig. 5. Nyquist plots of AISI 321 in 0.1 M H_2SO_4 solution after different immersion times: (a) 1 to 12 h and (b) 24 to 72 h.

have the same shape where a semicircle covers most the high-frequency region (f > 1 Hz) and a capacitive arc in the low-frequency domain. In Fig. 5(a), it is clear that the radius of the capacitive arc increases with the immersion time and it is related to the polarization resistance of the passive film. This reflects the growth of the surface film and an enhancement of its protective

behaviour as reported in literatures for stainless steel in alkaline media [19]. While, increasing of the radius of the capacitive arc with the immersion time is not observed in Fig. 5(b) as clear as in Fig. 5(a).

Literature proposes different models of equivalent circuits to interpret the impedance data on passive films formed on stainless steels.

64

Fig. 6. The fitting results of typical Nyquist plots of AISI 321 in 0.1 M H_2SO_4 solution after 3 h of immersion using the simplest equivalent circuit.

The simplest version consists in the modeling of the system with an equivalent circuit composed by one time constant as proposed by Pardo et al. [30] to describe the behaviour of AISI 304 and 316 stainless steels in H_2SO_4. In this circuit, as shown in Fig. 6, Rs is in a series with a parallel combination of Q_1 (double layer constant phase element) and R_1 (charge transfer resistance). Q_1 is used instead of pure capacitance to account for the depression of the capacitive loop which is usually attributed to surface heterogeneity [30]. However, as shown in Fig. 6 this model with one time constant could not fit the impedance data obtained in the present work.

The second version shown in Fig. 7 was utilized to represent the systems exhibit a

Table 2. Best fitting parameters for the impedance spectra of AISI 321 immersed in 0.1 M H_2SO_4 solution at different immersion times. $R_S = 7.5\ \Omega\ cm^2$

Time (h)	R_1 ($k\Omega\ cm^2$)	CPE_1 ($\mu\Omega^{-1}\ cm^{-2}\ s^{-n}$)	n_1	R_2 ($k\Omega\ cm^2$)	CPE_2 ($\mu\Omega^{-1}\ cm^{-2}\ s^{-n}$)	n_2	χ^2
1	0.975	134.1	0.854	43.365	941.4	0.664	0.077
3	1.592	167.8	0.819	128.655	893.9	0.706	0.075
6	1.635	146.2	0.831	178.875	781.8	0.725	0.083
12	1.575	137.1	0.833	208.260	749.4	0.738	0.085
24	4.323	111.4	0.853	114.505	923.2	0.758	0.052
48	4.925	107.2	0.856	95.527	961.6	0.763	0.064
72	5.251	115.2	0.849	90.232	985.1	0.749	0.068

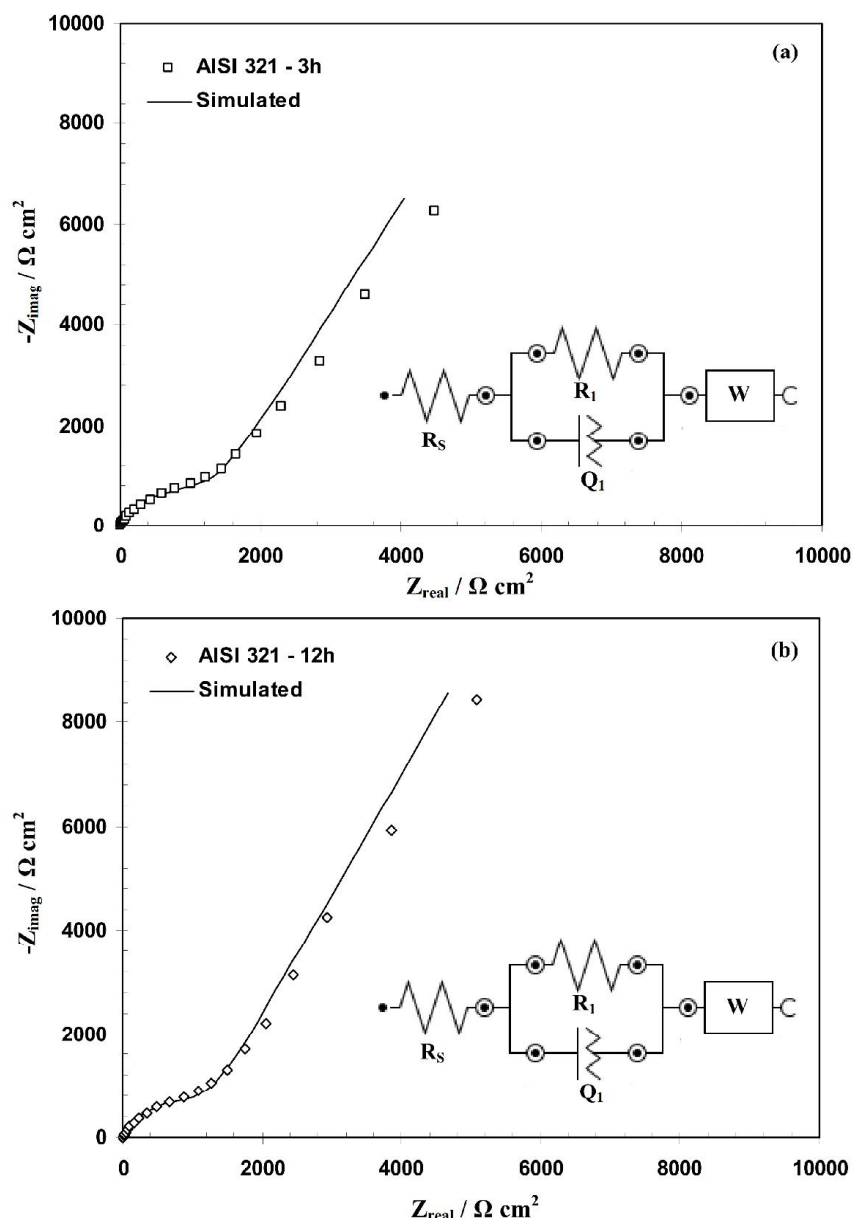**Fig. 7.** The fitting results of typical Nyquist plots of AISI 321 in 0.1 M H_2SO_4 solution after (a) 3 h and (b) 12 h of immersion using the second equivalent circuit.

capacitive loop followed by a straight line [31]. In this circuit, R_s is in a series with a parallel combination of Q_1 and R_1. W (Warburg impedance) represents the constant phase element due to the mass transfer process. This model also could not fit the impedance data obtained in the present study (Fig. 7).

The best version proposes an arrangement of two R-Q associations, as depicted in Fig. 8. This

equivalent circuit has been reported as excellent to model the passivation of stainless steels in acidic media [25, 32]. This circuit presents two time constants. The interpretation suggested for the circuit elements is the following one: the high-medium frequencies (R_1: charge transfer resistance, Q_1: double layer constant phase element) time constant can be associated with the charge transfer process and the low frequencies
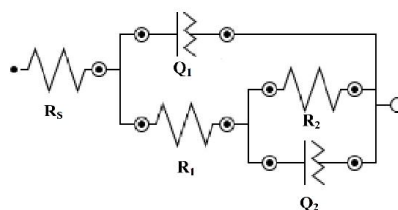
Fig. 8. The best equivalent circuit tested to model the experimental EIS data with two hierarchically distributed time constants.
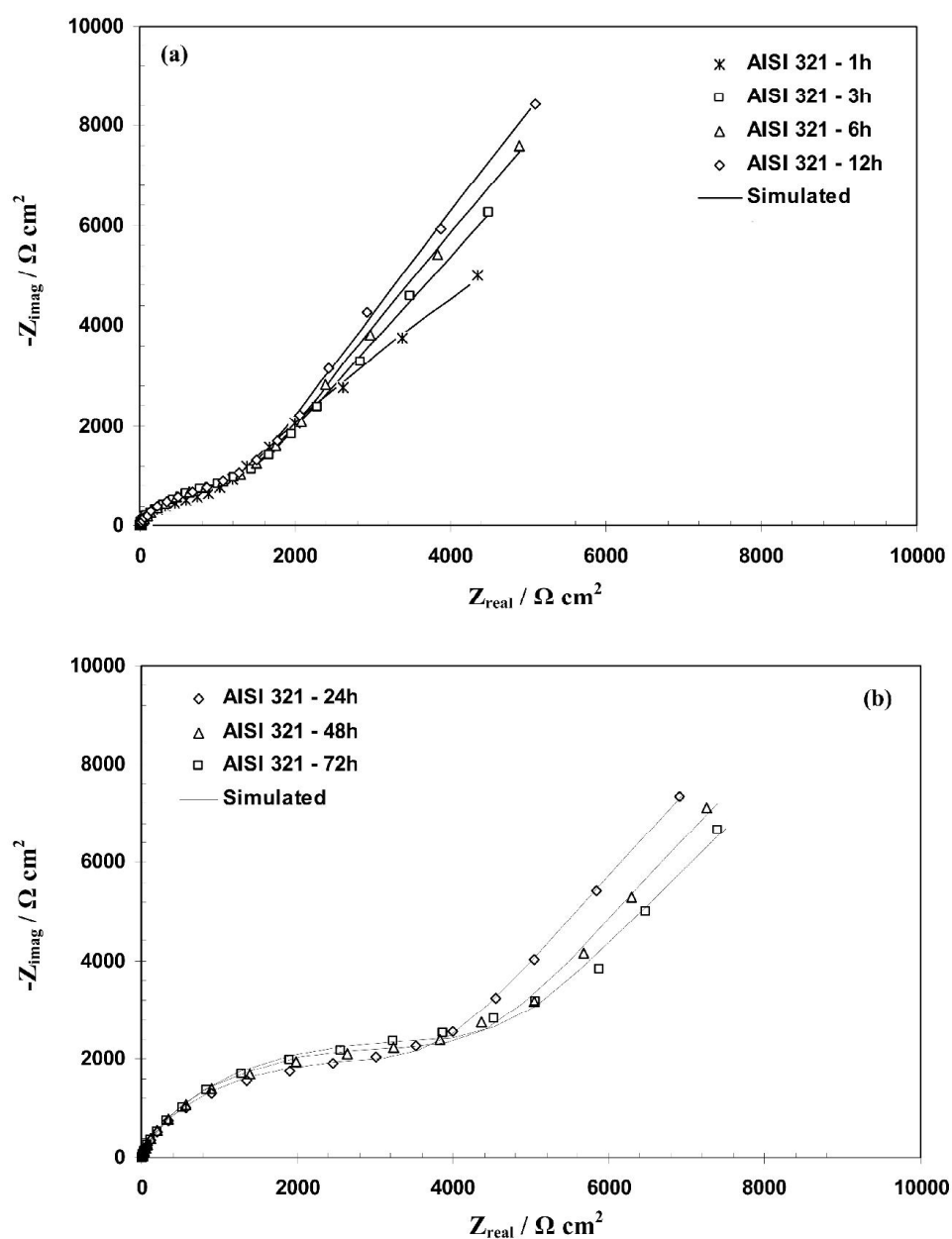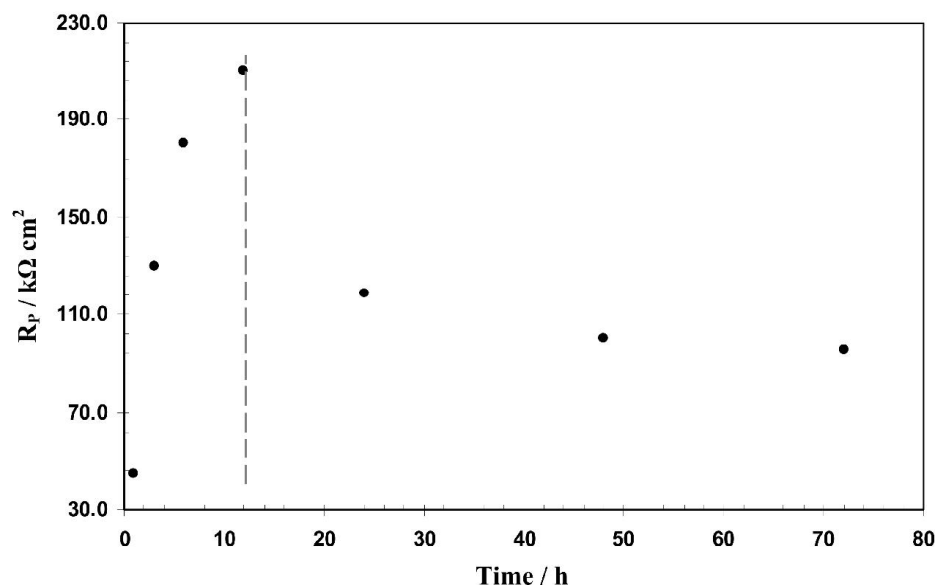

Fig. 9. The fitting results of Nyquist plots of AISI 321 in 0.1 M H_2SO_4 solution using the best equivalent circuit after different immersion times: (a) 1 to 12 h and (b) 24 to 72 h.

67

Fig. 10. Polarization resistance from the fitting procedure for AISI 321 in 0.1 M H_2SO_4 solution after different immersion times.

(R_2, Q_2) time constant can be correlated with the redox processes taking place in the surface film. This equivalent circuit was provided best fitting as shown in Fig. 9.

Table 2 presents the best fitting parameters obtained for the films formed on AISI 321 immersed in 0.1 M H_2SO_4 solution. Concerning the evolution with time, the fitting parameters R_1 and CPE_1 for the films formed on AISI 321 are little affected. R_1 suffers little increase, and the admittance of Q_1 seems very close to the values expected for a double layer capacitance. However, the fitting parameters R_2 and CPE_2 are affected by the immersion time. Initially, for 1 to 12 h: R_2 increases by about 2–4 times, with a tendency to increase with the immersion time, whereas CPE_2 decreases. At the sufficiently immersion time (t > 12 h): R_2 decreases and CPE_2 increases with the immersion time.

Polarization resistance, R_p ($R_p = R_1 + R_2$), where R_1 and R_2 were parameters from the fitting procedure, is commonly used as a measure of the resistance of a metal to the corrosion damage [19]. The calculated R_p for the passive films formed on AISI 321 immersed in 0.1 M H_2SO_4 solution is shown in Fig. 10. As shown, the polarization resistance initially increased with the

immersion time, 1 to 12 h, due to the establishment of the passive film layer. At the sufficiently immersion time (t > 12 h), the polarization resistance (interfacial impedance) is observed to decrease with increasing time. This variation of polarization resistance is fully accordance with corrosion current density.

4. CONCLUSIONS

The electrochemical behaviors of the passive film formed on AISI 321 in 0.1 M H_2SO_4 solution after different immersion times were investigated in the present work. Conclusions drawn from the study are as follows:

1. The polarization curves suggested that AISI 321 showed comparable passive behaviour in 0.1 M H_2SO_4 solution.
2. Mott–Schottky analysis revealed that the existence of a duplex passive film structure composed of two oxide layers of distinct semiconductivities (n-type and p-type).
3. Based on the Mott–Schottky analysis, it was shown that donor and acceptor densities are in the range of 1021 cm-3 and increased with the immersion time.
4. EIS results showed that the best electrical

68

equivalent circuit presents two time constants: The high medium-frequencies time constant can be correlated with the charge transfer process and the low frequencies time constant has been associated with the redox processes taking place in the surface film.

5. Based on the EIS analysis, it was shown that the polarization resistance (interfacial impedance) initially increased with the immersion time (1 to 12 h). This reflects the growth of the surface film and an enhancement of its protective behaviour. However, at the sufficiently immersion time (t > 12 h), the polarization resistance is observed to decrease with increasing time.

REFERENCES

1. Yamamoto, T., Fushimi, K., Seo, M., Tsuri, S., Adachi, T., and Habazaki, H., "Depassivation–repassivation behavior of type-312L stainless steel in NaCl solution investigated by the micro-indentation", Corros. Sci., 2009, 51, 1545.

2. Pardo, A., Merino, M. C., Coy, A. E., Viejo, F., Carboneras, M., and Arrabal, R., "Influence of Ti, C and N concentration on the intergranular corrosion behaviour of AISI 316Ti and 321 stainless steels", Acta Materialia, 2007, 55, 2239.

3. Chen, Y. Y., Liou, Y. M., and Shih, H. C., "Stress corrosion cracking of type 321 stainless steels in simulated petrochemical process environments containing hydrogen sulfide and chloride", Mater. Sci. Eng. A, 2005, 407,114.

4. Hakiki, N. E., Da Cunha Belo, M., Simões, A. M. P., and Ferreira, M. G. S., "Semiconducting properties of passive films on stainless steel. Influence of the alloying elements", J Electrochem. Soc., 1998, 145, 3821.

5. Sugimoto, K., and Sawada, Y., "The role of molibdenum additions to austenite stainless steels in the inhibition of pitting in acid chloride solutions", Corros. Sci., 1997, 17, 425.

6. Kong, D. S., Chen, S. H., Wang, C., and Yang, W., "A study of the passive films on chromium by capacitance measurement", Corros. Sci., 2003, 45, 747.

7. Kang, J., Yang, Y., Jiang, X., and Shao, H., "Semiconducting properties of passive films formed on electroplated Ni and Ni–Co alloys", Corros. Sci., 2008, 50, 3576.

8. Zhang, B., Li, Y., and Wang, F., "Observations of anomalies in the anodic behaviour of microcrystalline aluminium", Corros. Sci., 2010, 52, 2612.

9. Sellers, M. C. K., and Seebauer E. G., "Measurement method for carrier concentration in TiO_2 via the Mott–Schottky approach", Thin Solid Films, 2011, 519, 2103.

10. Zhang, G. A., and Cheng, Y. F., "Micro-electrochemical characterization and Mott–Schottky analysis of corrosion of welded X70 pipeline steel in carbonate/bicarbonate solution", Electrochim. Acta., 2009, 55, 316.

11. Amri, J., Souier, T., Malki, B., and Baroux, B., "Effect of the final annealing of cold rolled stainless steels sheets on the electronic properties and pit nucleation resistance of passive films", Corros. Sci., 2008, 50, 431.

12. Fattah-alhosseini, A., Farahani, H., "Electrochemical behaviour of AISI 304 stainless steel in sulfuric solution: Effects of acid concentration", Iranian Journal of Materials science and Engineering, 2014.

13. Taveira, L. V., Montemor, M. F., Da Cunha Belo, M., Ferreira, M. G., and Dick, L. F. P., "Influence of incorporated Mo and Nb on the Mott–Schottky behaviour of anodic films formed on AISI 304L", Corros. Sci., 2010, 52, 2813.

14. Cho, E. A., Kwon, H. S., and Macdonald, D. D., "Photoelectrochemical analysis on the passive film formed on Fe–20Cr in pH 8.5 buffer solution", Electrochim. Acta, 2002, 47, 1661.

15. Hakiki, N. E., Boudin, S., Rondot, B., and Da Cunha Belo, M., "The electronic structure of passive films formed on stainless steels", Corros. Sci., 1995, 37, 1809.

16. Rangel, C. M., Silva, T. M., and Da Cunha Belo, M., "Semiconductor electrochemistry approach to passivity and stress corrosion cracking susceptibility of stainless steels". Electrochim. Acta, 2005, 50, 5076.

17. Olsson, C. O. A., and Landolt, D., "Passive films on stainless steels: chemistry", structure and growth, Electrochim. Acta, 2003, 48, 1093.

18. Freire, L., Carmezim, M. J., Ferreira, M. G. S., and Montemor, M. F., "The passive behaviour of AISI 316 in alkaline media and the effect of pH: A combined electrochemical and analytical study", Electrochim. Acta, 2010, 55, 6174.

19. Luo, H., Dong, C. F., Li, X. G., and Xiao, K., "The electrochemical behaviour of 2205 duplex stainless steel in alkaline solutions with different pH in the presence of chloride", Electrochim. Acta, 2012, 64, 211.

20. Fattah-alhosseini, A., Soltani, F., Shirsalimi, F., Ezadi, B., and Attarzadeh, N., "The semiconducting properties of passive films formed on AISI 316 L and AISI 321 stainless steels: A test of the point defect model (PDM)", Corros. Sci., 2011, 53, 3186.

21. Bardwell, J. A., Sproule, G. I., MacDougall, B., Graham, M. J., Davenport, A. J., and Isaacs, H. S., "In Situ XANES Detection of Cr(VI) in the Passive Film on Fe-26Cr", J. Electrochem. Soc., 1992, 139, 371.

22. Dutta, R. S., Dey, G. K., and De, P. K., "Characterization of microstructure and corrosion properties of cold worked Alloy 800", Corros. Sci., 2006, 48, 2711.

23. Raja, K. S., and Jones, D. A., "Effects of dissolved oxygen on passive behavior of stainless alloys", Corros. Sci., 2006, 48, 1623.

24. Yang, Y., Guo, L. j., and Liu, H., "Effect of fluoride ions on corrosion behavior of SS304L in simulated proton exchange membrane fuel cell (PEMFC) cathode environments", J. Power Sour., 2010, 195, 5651.

25. Escrivà-Cerdán, C., Blasco-Tamarit, E., García-García, D. M., García-Antóna, J., and Guenbour, A., "Effect of potential formation on the electrochemical behaviour of a highly alloyed austenitic stainless steel in contaminated phosphoric acid at different temperatures", Electrochim. Acta, 2012, 80, 248.

26. Sato, N., "An overview of passivity of metals", Corros. Sci., 1990, 31, 1.

27. Ferreira, M. G. S., Hakiki, N. E., Goodlet, G., Faty, S., and Simoes, A. M. P., Da Cunha Belo, M., "Influence of the temperature of film formation on the electronic structure of oxide films formed on 304 stainless steel", Electrochim. Acta, 2001, 46, 3767.

28. Oguzie, E. E., Li, J., Liu, Y., Chen, D., Li, Y., Yang, K., and Wang, F., "The effect of Cu addition on the electrochemical corrosion and passivation behavior of stainless steels", Electrochim. Acta, 2010, 55, 5028.

29. Macdonald, D. D., "On the existence of our metals-based civilization I. Phase-space analysis", J. Electrochem. Soc., 2006, 153, B213.

30. Pardo, A., Merino, M. C., Carboneras, M., Viejo, F., Arrabal, R., and Munoz, J., "Influence of Cu and Sn content in the corrosion of AISI 304 and 316 stainless steels in H_2SO_4, Corros". Sci., 2006, 48, 1075.

31. Hermas, A. A., and Morad, M. S., "A comparative study on the corrosion behaviour of 304 austenitic stainless steel in sulfamic and sulfuric acid solutions", Corros. Sci., 2008, 50, 2710.

32. Metikoš-Hukovic, M., Babic, R., Grubac, Z., Petrovic, Z., and Lajçi, N., "High corrosion resistance of austenitic stainless steel alloyed with nitrogen in an acid solution", Corros. Sci., 2011, 53, 2176.

70